



Torsional brace strength requirements for steel I-girders

Yangqing Liu¹, Matthew C. Reichenbach², Todd A. Helwig³

Abstract

Torsional bracing is often used to stabilize beams in building and bridge applications. The bracing improves the stability by restraining twist of the cross section. Adequate stability bracing must satisfy both stiffness and strength requirements. The torsional brace strength requirements in the latest edition of the AISC specification (2016) was significantly changed from previous editions of the specification (2010). This paper outlines a parametric study on the strength requirements of beam torsional bracing. The paper demonstrates that the latest expression results in brace strength predictions that can be significantly unconservative. The paper recommends returning the strength provisions that were provided in previous editions of the specification.

1. Introduction

Lateral torsional buckling (LTB) is a limit state that may control the design of I-girder systems. The critical stage for LTB often occurs during placement of the concrete slabs since the non-composite steel girders support the entire construction load. The LTB resistance is improved by reducing the unsupported length of the beam utilizing bracing. Effective bracing can be achieved by either preventing lateral movement of the compression flange or by restraining twist of the beam. Bracing that restrains twist is aptly referred to as torsional bracing. Torsional braces occur in many forms including plate diaphragms, cross frames, or a transverse flexural member framing between adjacent beams. As demonstrated by Winter (1960), effective bracing must satisfy both strength and stiffness requirements. Winter developed a simple model that demonstrated the impact of imperfections and the stiffness that was provided on the brace strength requirements.

Winter's work primarily focused discrete/nodal bracing systems for columns and also made some simplifications to extend the method to beams. Although Winter's method focused on just discrete/nodal bracing, the fundamental concepts of stiffness and strength translate to all stability-related bracing systems.

The focus of this study is on torsional bracing of beams. There have been a number of previous

¹ Visiting Scholar at UT Austin, Tongji University, <1432232@tongji.edu.cn >

² Graduate Research Assistant, The University of Texas at Austin, <reichenbach.matt@utexas.edu>

³ Associate Chair, Professor, and J. Neils Thompson Centennial Teaching Fellowship in Civil Engineering, The University of Texas at Austin, <thelwig@mail.utexas.edu >

investigations on the behavior of torsional bracing, including the work of Taylor and Ojalvo (1966) who provided a solution for the LTB buckling capacity of beams with continuous torsional bracing that could be used to determine the required stiffness of the beam. Yura (2001) extended the solution for application with discrete torsional braces as well as a number of other variables including moment gradient, load position, and cross sectional distortion.

An important concept to understand with regards to bracing behavior is concept of the “ideal” stiffness, which is the brace stiffness that is required for a perfectly straight member to reach a specified load – which is often taken equal to the load corresponding to buckling between the brace points. The concept established by Winter (1960) and extended by Yura (2001) in the development of the bracing provisions in the AISC specification is to provide at least twice the ideal stiffness to control brace forces and deformations. For columns, Winter’s model demonstrated that the amount of deformation that will occur at a brace point is equal to the magnitude of the initial imperfection, when twice the ideal stiffness is provided. Therefore, the brace force is often taken as the brace stiffness multiplied by the magnitude of the initial imperfection. For torsional bracing systems, simplifications were applied to the stiffness formation outlined in Yura (2001) to produce the following required stiffness:

$$\beta_{Tbr} = \frac{2.4LM_r^2}{\phi nEI_{yeff}C_b^2} \quad (1)$$

wherein β_{Tbr} is the system torsional brace stiffness; L is the span length; M_r and n are the maximum factored moment and the number of intermediate braces within the span; I_{yeff} is the effective moment of inertia; ϕ is the resistance factor; and C_b is the moment gradient factor assuming the beam buckles between the brace points. Prior to the 2016 AISC specification, the brace strength requirement was given by the following expression:

$$M_{br} = \beta_T \theta_0 = \frac{0.024M_r L}{nC_b L_b} \quad (2)$$

Equation (2) is based upon the assumption that twice the ideal stiffness was provided so that the twist at the brace was equal to the initial imperfection. Additional simplifications were applied as outlined in the AISC Commentary (2010) were applied. The expression also is based upon the assumption that the section has the critical shape initial imperfection. Wang and Helwig (2005) demonstrated that the critical shape imperfection for torsional bracing consists of a lateral sweep of the compression flange equal to $L_b/500$ (sweep tolerance) and the tension flange is straight, producing an initial twist equal to $L_b / 500h_0$ where L_b and h_0 are the respective unbraced length and distance between flange centroids. The latest AISC Specification (2016) included a change in the torsional brace moment based on the recommendations from Prado and White (2015). Prado and White (2015) carried out a detailed investigation on the stability bracing requirements including the behavior in the inelastic region. The study was focused heavily on the requirements to reach the plastic bending strength for beams with relatively short unbraced lengths and resulted in the following torsional brace moment:

$$M_{br} = 0.02M_r \quad (3)$$

Where, M_r is the design moment in the beam. Although the simplicity of Equation (3) is attractive, the applicability of the expression for general design situations is questionable. In

particular, beams with unbraced lengths at or near the elastic buckling limit can experience significantly larger brace moments than 2% of the design moment.

This paper focuses on the brace strength requirements of steel beams with torsional braces. The applicability of Equations (2) and (3) for the general stability design requirements of steel beams is covered. The paper begins by providing background information that is necessary to understand the fundamental behavior of torsional bracing systems. The results from a parametric study on the torsional bracing behavior of beams are covered including the effects of material inelasticity and the number of intermediate braces. Finally, recommendations are made for the strength requirements of torsional braced beams.

2. Background

There are a number of factors that impact the stiffness behavior of bracing systems. For torsional bracing of beams, there are three primary stiffness components: 1) brace stiffness, β_b ; 2) cross-sectional distortion, β_{sec} , and 3) in-plane stiffness of the beams, β_g . Most bracing systems tend to follow the expression for springs in series (Yura, 1992), resulting in the following expression for the system torsional brace stiffness, β_T :

$$\frac{1}{\beta_T} = \frac{1}{\beta_b} + \frac{1}{\beta_{sec}} + \frac{1}{\beta_g} \quad (4)$$

The nature of Eq. (4) is such that β_T is smaller than the smallest of the three components. From a design perspective, for a given bracing system, the system stiffness given by Eq. (4) must be larger than the stiffness requirement from Eq. (1). Therefore, from a behavioral perspective, failure can occur if any of the three stiffness components in Eq. (4) are less than that stiffness required given by Eq. (1). Although this previous statement may seem obvious, there have been a number of near failures of torsional braced beams because the in-plane stiffness, β_g , is often overlooked. The impact of in-plane girder stiffness on the effectiveness of torsional bracing was first documented by Helwig (1993) through investigating twin-girder systems. The internal force components developed in a cross-frame include shears that act upward on one girder and downward on the other girder. The shears and corresponding girder deformation can lead to a rigid-body rotation of the systems that dramatically decreases the effectiveness of torsional bracing. They also put forward the following Eq. (5) for the in-plane stiffness of twin girders, which was later extended to Eq. (6) (Yura et. al, (1993), Helwig and Yura (2015)) for systems containing more than two girders, where S and I_x are the respective girder spacing and the in-plane moment of inertia; and n_g is the number of girders across the width of the system.

$$\beta_g = \frac{12S^2EI_x}{L^3} \quad (5)$$

$$\beta_g = \frac{24(n_g - 1)^2 S^2 EI_x}{n_g L^3} \quad (6)$$

The in-plane stiffness effect (β_g) is mainly important on systems with a relatively narrow width compared to the span, such as two- and three-girder systems. The AISC specification includes expressions for β_b and β_{sec} that have been shown to produce good predictions on the behavior. Because many building systems tend to have significant width across the width compared to the span, the in-plane stiffness component (β_g) was not included in the AISC bracing provisions.

However, the collapse of the Marcy Pedestrian Bridge (unbraced tub girder) as well as near-collapses of several narrow 2- and 3-girder systems exposed the profession to a mode of buckling that is often referred to as the “system mode of buckling” outlined in Yura et al. (2008).

$$M_{gs} = \frac{\pi^2 SE}{L^2} \sqrt{I_{yeff} I_x} \quad (7)$$

From a general behavioral perspective, the system mode of buckling given by Eq. (7) will typically control when the in-plane stiffness (β_g) is less than the torsional brace stiffness required given by (1). The mode of buckling is not generally sensitive to the brace stiffness or spacing. Improving the behavior requires changes in the girder geometry or additional restraints from lateral bracing. Additional work has recently been carried out in Han and Helwig (2016) to extend the application of the above expression considering the impact of moment gradient, girder continuity, second order effects, and the impact of imperfections on the mode. Although the system effect outlined in Eq. (7) may appear relatively involved compared to torsional bracing moment behavior discussed in this paper, understanding the basic behavior of the mode is important with respect to the finite element modelling decisions that are outlined in the next section.

3. Finite – Element Model

To investigate the torsional brace strength behavior, parametric finite element analyses was carried out on twin I-girder systems using ABAQUS (2017). The cross sections of the girders were modelled using shell elements. The torsional braces consisted of cross frames that framed between the two adjacent girders. Cross frames are commonly used in bridges and in some building applications. The cross frames were modelled by the linear truss element T3D2. The cross frames shared nodes located at the flange to web juncture at the top and bottom of the I-sections. Because the torsional braces were “full-depth” there was no cross sectional distortion associated with web flexibility. The girders were with the 4-node full integration shell element S4. The shell elements were square with a mesh size of 2 in. (50.8 mm). Three different cross sections were considered in the study as depicted in Fig. 2. The span of the girders was equal to 100 ft. (30.48 m). Since the three girders had a web depth of 48 in. (1.219 m), the span-to-depth ratio L/d was 25, which is representative of beams used in practice. A web thickness of 0.75 in. (19.05 mm) was used for all the girders to maintain a relatively stocky web and avoid local buckling in the web. The thickness of the flanges were selected to give a compact flange with a width/thickness ratio of 8, which is compact for grade 50 steel and therefore avoided local flange buckling. The flange sizes of the three sections provided flange width to depth ratios of 1/6, 1/4, and 1/3. The value of 1/6 is the extreme limit allowed in the AASHTO bridge specification (2016), while the value of 1/3 is consistent with many rolled sections.

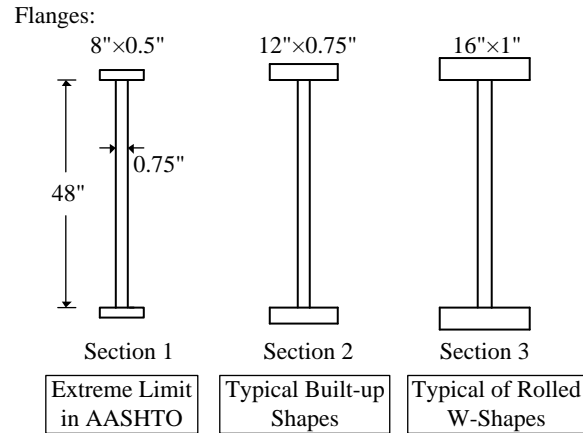


Figure 1: Cross sections considered in parametric study

The number of braces provided on the beams ranged from 1 to 5, resulting in unbraced lengths ranging from 50 ft. (15.24 m) to 16.67 ft. (5.08 m). To avoid issues with system buckling discussed in the previous section, the girder spacing ranged from 20 ft. (6.10 m) to 30 ft. (9.14 m). The larger spacing of 30 ft. (9.14 m) was required for cases with a larger number of intermediate braces to improve the system mode buckling capacity so that it didn't control over buckling between the brace points. Fig. 3 shows the layout and boundary conditions of the twin-girder systems. Both elastic and inelastic analyses are carried out in this paper. In the inelastic analysis, the elastic perfectly plastic steel constitution is employed for the girders. However, sometimes the simulation cannot converge because of the stress concentration at the end of girders. Therefore, the ends of girders with a length of 12 in. (0.30 m) in the models use the elastic material. The in-plane boundary conditions of the twin-girders consist of the simple support at the mid-height points of cross sections. Twist was restrained at the ends of the girders by stopping lateral movement at the top and bottom of the webs. The sections were free to warp at the supports.

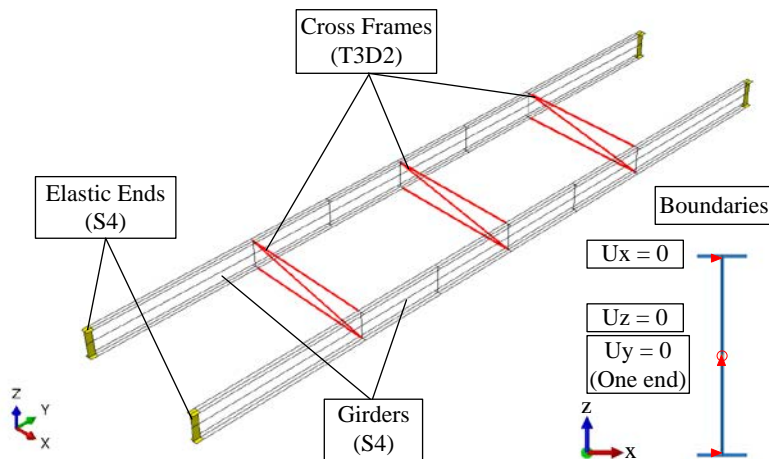


Figure 2: Layout and boundary conditions of twin-girder systems

As for initial imperfections, Wang and Helwig (2005) showed that the critical shape imperfection for beam torsional bracing consists of a lateral sweep of compression flange while the tension flange remains straight. The distribution of the imperfection along the length was the same as

utilized by Prado and White (2015) which consists of an asymmetric initial imperfection shape is applied on the top flanges by forced lateral displacements, as depicted in Fig.5.

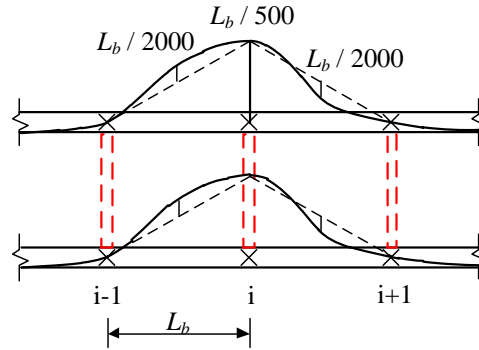


Figure 3: Initial imperfection shape

The critical segment for buckling was always the section near midspan where the moment was the largest. In cases with more than 1 brace, the critical segment often received warping restraint from the adjacent segments with lower moment levels. To avoid accounting for the warping restraint on the buckling capacity, Timoshenko's buckling solution for a doubly-symmetric section was used to identify the moment level corresponding to buckling between the brace points:

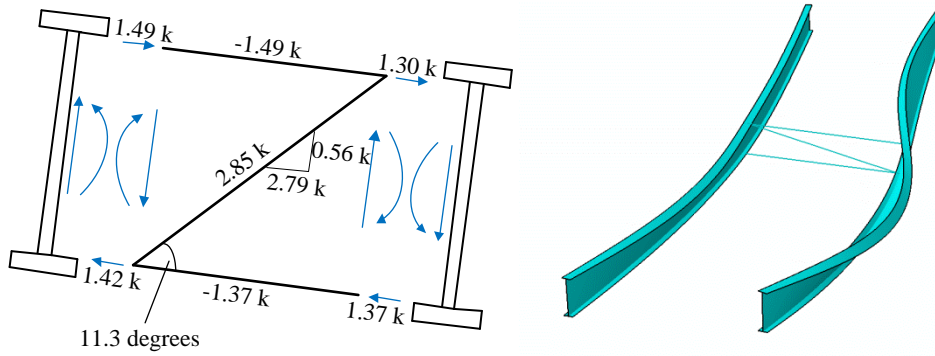
$$M_{cr} = \frac{\pi}{L_b} \sqrt{EI_y GJ + E^2 I_y C_w \frac{\pi^2}{L_b^2}} \quad (8)$$

where, L_b is the spacing between cross frames, J is the torsional constant, C_w is the warping constant, E is the elastic modulus, and G is the elastic shear modulus. Eigenvalue buckling analyses were conducted to obtain the ideal stiffness requirements of the bracing to reach the corresponding moment level. The ideal stiffness was determined as the stiffness required to reach the moment level corresponding to buckling between the brace points using Eq. (8). For all the analysis, twice the ideal stiffness was provided, matching the current assumption in the AISC provisions.

4. Finite – Element Results

Prior to the discussion of the strength behavior of torsional braces, an overview of how the brace moments were calculated is warranted. Table 1 shows the brace forces for an analysis on Section 2 for the case with a single cross frame at midspan for various load levels M/M_{cr} . The brace moments are sketched for the case $M/M_{cr} = 75\%$ in Fig. 6. As the system deforms, shears develop at the interface between the girder and the brace. One girder has an upward shear, while the other has a downward shear. The shears cause the moment in the girder on the left to be larger than moment in the girder on the right. Wang and Helwig (2005) showed that the cross frame forces are a function of the girder moment. In this case, because the girder on the left has a higher moment, the brace force is higher than the brace moment for the girder on the right. An idealized maximum and minimum force couple can be obtained from the strut forces. For example, the maximum value would be the top strut force multiplied by the depth of the brace as $1.49 \text{ k} \times 48 \text{ in.} = 71.5 \text{ k}\cdot\text{in.}$ (8.08 kN·m). The minimum is $1.37 \text{ k} \times 48 \text{ in.} = 65.8 \text{ k}\cdot\text{in.}$ (7.43 kN·m), and the average is $68.7 \text{ k}\cdot\text{in.}$ (7.76 kN·m). In design, an engineer would normally have

“equal” girder design moments from a first-order analysis, and therefore the average force is used in all graphs throughout this paper. In reality, one girder will have a higher brace moment and the other girder will have a smaller brace moment. The relative difference in the brace moments will generally be significant for twin girder systems and become smaller for wider systems with more girders.



(a) Forces and moments (b) Failure mode

Figure 4: A brace moment example

Table 1: Brace forces under various girder moments

M / M_{cr}	$F_{b,top}$ /kips	$F_{b,bot}$ /kips	$F_{b,diag}$ /kips	$M_{b,max}$ /(kips·in)	$M_{b,min}$ /(kips·in)	$M_{b,avg}$ /(kips·in)
0.25	0.15	0.15	0.30	7.20	6.99	7.09
0.50	0.55	0.52	1.06	26.27	24.95	25.61
0.75	1.49	1.37	2.85	71.54	65.75	68.64
1.00	5.31	4.65	9.89	254.90	223.10	239.00

* $M_b = F_b \cdot d$, d is the depth of bracing and girders.

Before general results are shown for all three sections, a discussion of the behavior for cases with elastic and inelastic material response is warranted. In the graphs of applied load versus brace moments, the applied load is normalized by the critical buckling moment (M_{cr}) using Eq. 8 whereas the brace moments are normalized by the applied moment (M). Fig. 7 shows a graph of the normalized applied moment versus the corresponding brace moment for Section 2 with 5 intermediate braces for the case with uniform moment loading. Four curves are shown corresponding to cases with an elastic material and inelastic material limits. The inelastic material limits correspond to $f_y = 36$ ksi, 50 ksi, and 70 ksi (248, 345 and 483 MPa). The curves are essentially coincident up until the cases with inelastic limits exhibit yielding in the material. The curves then diverge from one another and the cases with inelastic materials reach a maximum strength corresponding to plastification of the cross section. Although the maximum brace moments for these cases with inelastic materials are smaller than the case with elastic materials, the comparison is not significant since the analyses were controlled by different limit states. The case with elastic materials were controlled by stability with the beam supporting larger applied moments and experiencing more significant buckling related deformations. Many of the cases considered by Prado and White (2015) had a relatively short unbraced length and were controlled by plastification of the cross section assuming Gr. 50 steel. Tailoring the stability brace moments around a specific material yield strength can result in unconservative predictions

of the stability brace moments since the problem is not controlled by stability but is instead limited by cross sectional strength. The provisions for brace strength should consider the number of intermediate brace points and be applicable for cases with both larger and smaller unbraced lengths. Subsequent results of the brace strength demonstrate solutions with both elastic and inelastic materials. The inelastic material solutions used an arbitrary yield strength of 50 ksi (345 MPa). These results are mainly shown as an indicator for when yielding with a common grade of steel would control.

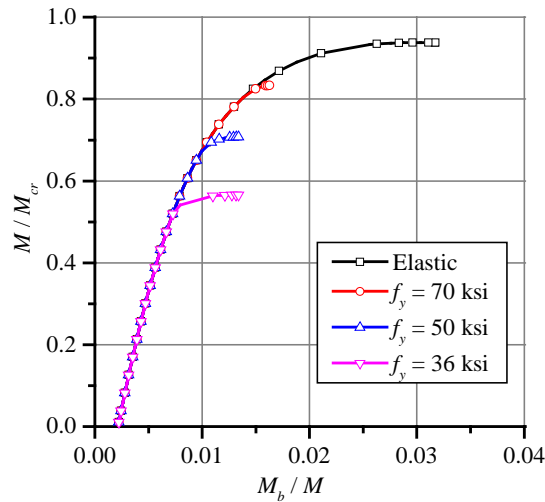


Figure 5: Brace moments under varying material limits

Fig. 8 shows the brace moments under uniform moment loading for all three sections that were considered. This observation is consistent with the study presented in Wang and Helwig (2005) that found the brace force is a function of the moment in the girder at the brace location. Three cases are graphed using an elastic analysis in addition to the one case is shown utilizing a material with an inelastic material ($f_y = 50 \text{ ksi} = 345 \text{ MPa}$) for the case of $n=5$. Although inelastic materials were also considered for $n=1$, and $n=3$, the curves were not significantly different than the elastic cases except at very large deformations when P-delta effects led to yielding of the section. For all three sections, considering the cases with elastic materials, the relative magnitude of the brace forces at the maximum girder moments decrease with an increase in the number of intermediate braces. The relative change in brace force tends to decrease as more braces are added (i.e. There is a large reduction going from $n=1$ to $n=3$, but the reduction is smaller going from $n=3$ to $n=5$). Some of the analyses did not reach convergence beyond 90~98% of M_{cr} for the cases with $n=3$ and $n=5$ due to excessive girder deflections. However, this level of convergence is reasonable since it is within the resistance factor ($\phi=0.9$) and provides a representative level of the bracing moment. The curve for inelastic materials with $n=5$ had smaller brace moments than the cases with elastic materials, which is consistent with the observations outline for Fig. 6. As noted in the earlier discussion, the sections were controlled by the limit state of cross sectional yielding and the results are not representative of the limit state for stability bracing. As a result, all subsequent results presented in the paper focus on elastic materials since such conditions are more critical than cases with inelastic materials. Finally, a comparison of the brace moments for the three different sections show that the magnitude of the brace moments in descending order are for Section 1, Section 2, and Section 3, which indicates

As noted earlier, the expression given in Eq. 3 was based upon analyses by Prado and White (2015) with closely spaced braces and the sections were generally controlled by the cross section capacity and not stability. The expression in Equation 2 was based upon generally elastic behavior as well as the assumption that at least twice the ideal stiffness was provided leading to a twist at the brace point equal to the initial imperfection of the section. Equation 2, can be treated to obtain an estimate of the behavior as a function of the required design moment for comparisons with the 2% in the current AISC equation. For cases with moment gradient and several braces, the moment gradient factor (C_b) tends 1.0 since the critical unbraced segment near the maximum moment has a relatively uniform moment diagram. In addition, the unbraced length can be expressed as a function of the number of intermediate braces using the expression:

$$L_b = \frac{L}{n} \quad (9)$$

Inserting $C_b = 1.0$ and Eq. 9 into Eq. 2 produces the following expression:

$$M_{br} = \frac{0.024M_r(n+1)}{n} \quad (10)$$

Considering different numbers of intermediate bracing, the following Table 3 can be generated:

Table 3: Results of Equation 10

n	1	2	3	4	5	...	10
M_{br} / M_r	0.048	0.036	0.032	0.030	0.029	...	0.026

The expression that was included in past AISC specifications tends to a practical minimum value of $2.6\%M_r$. Although significantly larger values than 0.048 were achieved in the FEA studies presented in this paper, the past expression better follows the observed trend that the brace moments are a function of the number of intermediate braces with the brace moment decreasing for additional braces. One of the reasons the expression underestimates the force is related to the assumption that providing a stiffness of twice the ideal stiffness results in a deformation at the brace equal to the magnitude of the initial imperfection, θ_0 . Although the assumption of providing twice the ideal stiffness limits the deformation to a value equal to the initial imperfection has been shown to work well with columns, the assumption does not work as well with beams; however it does provide reasonable estimates of the brace moment. Additional work was undertaken in the study presented herein on the stiffness required to limit the deformation to a value equal to the initial imperfection, which will be covered in a different paper.

5. Summary

This paper conducts a parametric study on the strength requirement of beam torsional bracing. The considered influential factors include the cross section, the intermediate bracing number, and the material inelasticity. The results show that when inelastic strength controls track along the elastic curves, the limit state is controlled by the cross sectional capacity. The lateral and torsional deformations are smaller since stability is not as critical. The torsional bracing moments are higher than 2% of the girder moments even if the girder moments are 90% of M_{cr} in some cases. The results demonstrate that the latest expression significantly underestimates the brace

moment resulting in unconservative strength predictions. The paper recommends returning the strength provisions that were provided in previous editions of the specification.

References

- Abaqus/CAE (2017). "Abaqus/CAE User's Guide."
- American Association of State Highway and Transportation Officials (2017). "LRFD Bridge Design Specifications (8th ed.)". Washington, D.C.
- American Institute of Steel Construction (2010). "Specification for Structural Steel Buildings." Chicago, IL
- American Institute of Steel Construction (2016). "Steel Construction Manual." Chicago, IL
- Han, L., and Helwig, T. (2016) "Effect of Girder Continuity and Imperfections on System Buckling of Narrow I-Girder Systems." Proceedings of the Structural Stability Research Council / North American Steel Construction Conference. Orlando.
- Helwig, T., Yura J. and Frank K. (1993) "Bracing Forces in Diaphragms and Cross Frames." Proceedings Structural Stability Research Council Conference, Milwaukee, WI. 129–140.
- Helwig, T., Yura J. (2015) Bracing System Design. Steel Bridge Design Handbook, Publication No. FHWA-HIF-16-002, Vol. 13, U.S. Department of Transportation Federal Highway Administration.
- Prado, E. and White, D. (2015). "Assessment of Basic Steel I-Section Beam Bracing Requirements by Test Simulation." Report to the Metal Building Manufacturers Association.
- Taylor, A. C. and Ojalvo, M. (1966). "Torsional Restraint of Lateral Buckling." J. Struct. Div., 92, 115–129.
- Timoshenko, S., and Gere, J. (1961). Theory of Elastic Stability, McGraw Hill, New York.
- Trahair, N. S. (1993). Flexural-Torsional Buckling of Structures. Vol. 6. CRC Press.
- Wang, L., & Helwig, T. A. (2005). "Critical Imperfections for Beam Bracing Systems." J. Struct. Eng., 131(6), 933–940.
- Winter, G. (1960). "Lateral Bracing of Columns and Beams." Trans. Am. Soc. Civ. Eng., 125, 809–825.
- Yura, J. A., Philip B., et al. (1992) Bracing of Steel Beam in Bridges. Research Report 1239-4F. Austin.
- Yura, J. A. (2001). "Fundamentals of Beam Bracing." Eng. J., 11–26.
- Yura, J., Helwig, T., Herman, R., & Zhou, C. (2008). "Global Lateral Buckling of I-Shaped Girder Systems." J. Struct. Eng., 134(9), 1487-1494.